

NASA Technical Memorandum 105768
ICOMP-92-11; CMOTT-92-07

IN-34

117607

p-23

A New Time Scale Based k - ϵ Model for Near Wall Turbulence

Z. Yang and T.H. Shih
*Institute for Computational Mechanics in Propulsion
and Center for Modeling of Turbulence and Transition
Lewis Research Center
Cleveland, Ohio*

(NASA-TM-105768) A NEW TIME SCALE
BASED K-EPSILON MODEL FOR NEAR WALL
TURBULENCE (NASA) 23 P

N92-32868

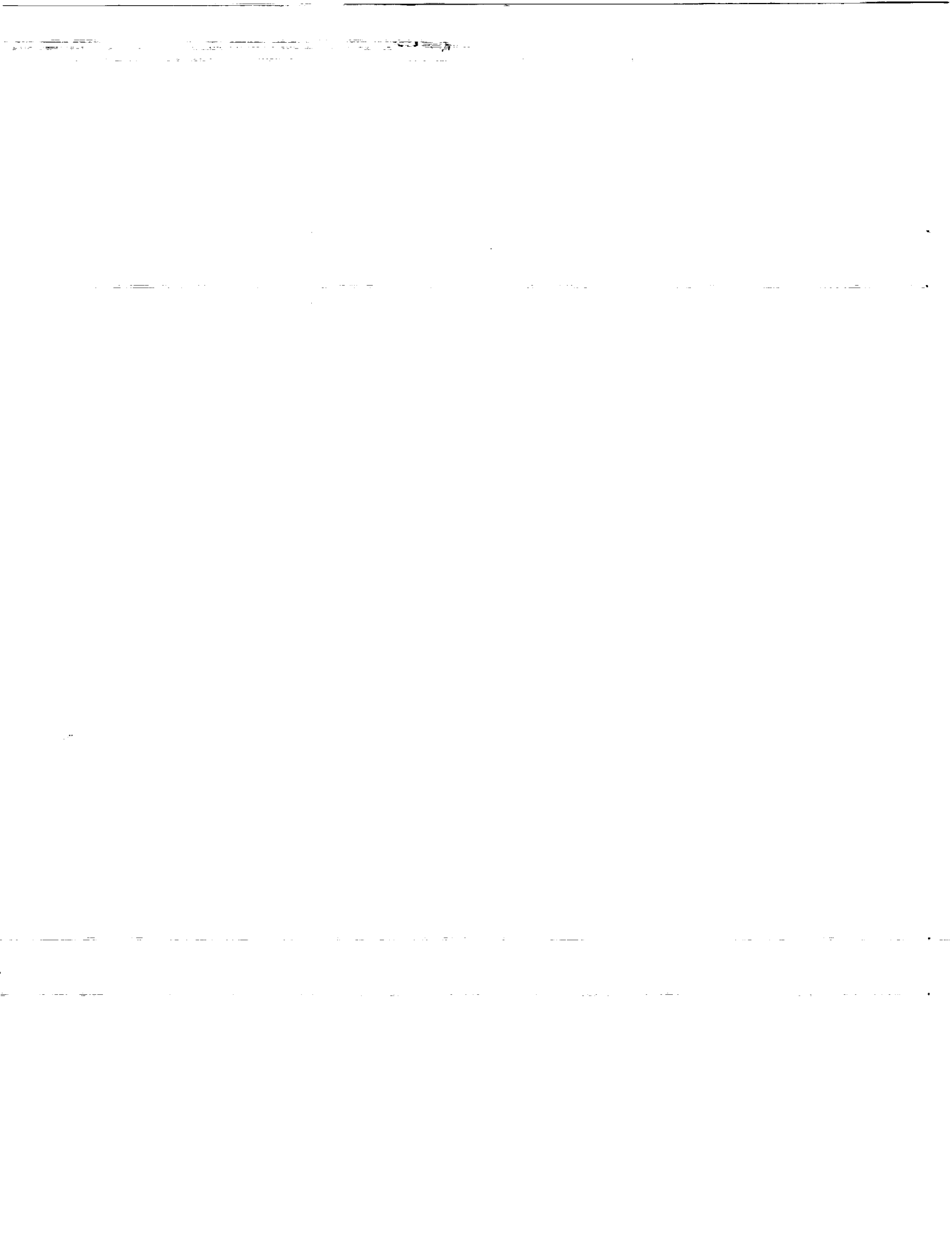
Unclass

G3/34 0117607

September 1992

NASA





A New Time Scale Based $k - \epsilon$ Model for Near Wall Turbulence

Z. Yang and T.H Shih

Center for Modeling of Turbulence and Transition

ICOMP/NASA Lewis Research Center

Cleveland, OH 44135

ABSTRACT

A $k - \epsilon$ model is proposed for wall bounded turbulent flows. In this model, the eddy viscosity is characterized by a turbulent velocity scale and a turbulent time scale. The time scale is bounded from below by the Kolmogorov time scale. The dissipation equation is reformulated using this time scale and no singularity exists at the wall. The damping function used in the eddy viscosity is chosen to be a function of $R_y = \frac{k^{1/2} y}{\nu}$ instead of y^+ . Hence, the model could be used for flows with separation. The model constants used are the same as in the high Reynolds number standard $k - \epsilon$ model. Thus, the proposed model will be also suitable for flows far from the wall. Turbulent channel flows at different Reynolds numbers and turbulent boundary layer flows with and without pressure gradient are calculated. Results show that the model predictions are in good agreement with direct numerical simulation and experimental data.

I. INTRODUCTION

In turbulence modeling, the $k - \epsilon$ model is the most widely used model in engineering calculations. The Standard $k - \epsilon$ Model^{1,2} was devised for high Reynolds number turbulent flows and is traditionally used in conjunction with a wall function when it is applied to wall bounded turbulent flows. However universal wall functions do not exist in complex flows and it is thus necessary to develop a form of $k - \epsilon$ model equations which can be integrated down to the wall.

Jones and Launder³ were the first to propose a low Reynolds number $k - \epsilon$ model for near wall turbulence, which was then followed by a number of similar $k - \epsilon$ models. A critical

evaluation of the pre-1985 models was made by Patel et al.⁴. More recently proposed models are found in Shih⁵ and Lang and Shih⁶. Three major deficiencies can be pointed out about existing $k - \epsilon$ models. (Some of the models may have only one or two of the three deficiencies.) First, a near wall pseudo-dissipation rate was introduced to remove the singularity in the dissipation equation at the wall. The definition of the near wall pseudo-dissipation rate was quite arbitrary. Second, the model constants were different from those of the Standard $k - \epsilon$ Model, making the near wall models less capable of handling flows containing both high Reynolds number turbulence and near wall turbulence, which is often the case for a real flow situation. Patel et al.⁴ put as the first criterion the ability of the near wall models to be able to predict turbulent free shear flows. Third, the variable y^+ is used in the damping function f_μ of the eddy viscosity formulae. Since the definition of y^+ involves u_τ , the friction velocity, any model containing y^+ can not be used in flows with separation.

In this paper, a new time scale based $k - \epsilon$ model for near wall turbulence is proposed. In this model, $k^{1/2}$ is chosen as the turbulent velocity scale. The time scale is bounded from below by the Kolmogorov time scale. When this time scale is used to reformulate the dissipation equation, there is no singularity at the wall and the introduction of a pseudo-dissipation rate is avoided. The model constants are exactly the same as those in the Standard $k - \epsilon$ Model, that ensures the performance of the model far from the wall. A damping function is proposed as a function of $R_y = \frac{k^{1/2} y}{\nu}$ instead of y^+ . Thus, the present model can be used for separated flows. The performance of the model is then tested against turbulent channel flows at different Reynolds numbers and turbulent boundary layer flows at zero pressure gradient, favorable pressure gradient, adverse pressure gradient, and increasingly adverse pressure gradient. The results of the model prediction are compared with available data from direct numerical simulations and experiments.

II. NEAR WALL $k - \epsilon$ MODEL

In turbulence modeling, the instantaneous quantities of an incompressible flow are decomposed into the mean and the fluctuating parts, i.e., $\bar{u}_i = U_i + u_i$, $\bar{p} = P + p$. The mean

field U_i satisfies the following continuity equation and Reynolds averaged Navier-Stokes equation:

$$U_{i,i} = 0 \quad (1)$$

$$\dot{U}_i + U_j U_{i,j} = -\frac{1}{\rho} P_i + \nu U_{i,jj} - \langle u_i u_j \rangle_{,j} \quad (2)$$

where the Reynolds stress term, $-\langle u_i u_j \rangle$, must be modeled.

In an eddy viscosity model, one assumes mean field by

$$-\langle u_i u_j \rangle = \nu_T (U_{i,j} + U_{j,i}) - \frac{2}{3} k \delta_{ij}, \quad (3)$$

where ν_T is the eddy viscosity and k is the turbulent kinetic energy. From dimensional reasoning, the eddy viscosity is given by

$$\nu_T \sim u_t l_t, \quad (4)$$

where u_t and l_t are the turbulent velocity scale and turbulent length scale, respectively. In the framework of a high Reynolds number $k - \epsilon$ model, $u_t \sim k^{1/2}$, $l_t \sim \frac{k^{3/2}}{\epsilon}$ (which gives the turbulent time scale $T_t \sim \frac{k}{\epsilon}$), and the resulting eddy viscosity is given by

$$\nu_T = c_\mu \frac{k^2}{\epsilon} \quad (5)$$

The transport equations for k and ϵ are modeled as

$$\dot{k} + U_j k_{,j} = [(\nu + \frac{\nu_T}{\sigma_k}) k_{,j}]_{,j} - \langle u_i u_j \rangle U_{i,j} - \epsilon \quad (6)$$

$$\begin{aligned} \dot{\epsilon} + U_j \epsilon_{,j} &= [(\nu + \frac{\nu_T}{\sigma_\epsilon}) \epsilon_{,j}]_{,j} - C_{1\epsilon} \langle u_i u_j \rangle U_{i,j} \frac{\epsilon}{k} - C_{2\epsilon} \frac{\epsilon^2}{k} \\ &= [(\nu + \frac{\nu_T}{\sigma_\epsilon}) \epsilon_{,j}]_{,j} + (-C_{1\epsilon} \langle u_i u_j \rangle U_{i,j} - C_{2\epsilon} \epsilon) / T_t \end{aligned} \quad (7)$$

Equations (5), (6), (7) with the following values of the constants $c_\mu = 0.09$, $C_{1\epsilon} = 1.44$, $C_{2\epsilon} = 1.92$, $\sigma_k = 1.0$, $\sigma_\epsilon = 1.3$ are commonly referred to as the Standard $k - \epsilon$ Model^{1,2}.

A singularity would appear if the Standard $k - \epsilon$ Model were applied down to the wall because of vanishing k at the wall, which renders the time scale $T_t (= k/\epsilon)$ in equation (7)

zero. However, as we shall show later, k/ϵ can not represent the turbulent time scale near the wall. As the wall is approached, this commonly used time scale must be modified.

The turbulent length scale is characterized by the size of the energy containing eddies. Near the wall, these eddies would have a size of $O(y)$. Following Hanjalic and Launder⁷, the turbulent velocity field has the following expansions near the wall:

$$\begin{aligned} u' &= a_1 y + a_2 y^2 + \dots \\ v' &= b_2 y^2 + \dots \\ w' &= c_1 y + c_2 y^2 + \dots \end{aligned} \quad (8)$$

where a_1, b_2, c_1 are non-zero in general. Thus, as the wall is approached, both the turbulent length scale and the turbulent velocity scale approach zero. However, the turbulent time scale, which is given by the ratio of the length scale of the energy containing eddies to the turbulent velocity scale, approaches a non-zero value. We expect that this time scale must be the Kolmogorov time scale because viscous dissipation dominates near the wall. Thus, the turbulence time scale is given by k/ϵ away from the wall and by the Kolmogorov time scale near the wall. Since k/ϵ is much larger than the Kolmogorov time scale away from the wall and k/ϵ vanishes near the wall due to the boundary condition on k , we can simply write

$$T_t = \frac{k}{\epsilon} + T_k \quad (9)$$

where

$$T_k = c_k \left(\frac{\nu}{\epsilon}\right)^{1/2} \quad (10)$$

is the Kolmogorov time scale and c_k is a constant of order one. In the present investigation, $c_k = 1.0$ is used. The constant c_k was varied from 0.5 to 3.0 and the solutions were found to be quite insensitive to c_k in this range. As more flow situations are tested, the value of c_k could be optimized by fine tuning.

Now the time scale given by equation (9) is bounded from below by the Kolmogorov time scale which is always positive. When this time scale is used in equation (7), there will

be no singularity at the wall. The argument on the time scale for near wall turbulence and the method to remove the singularity in the dissipation equation at the wall are also used by other researchers, see Durbin⁸, for example.

If we use $k^{1/2}$ as the turbulent velocity scale and use the turbulent time scale as given by equation (9), the turbulent length scale is then the velocity scale times the time scale. Hence the eddy viscosity can be written as

$$\nu_T = c_\mu f_\mu k T_t \quad (11)$$

where f_μ is the damping function which is used to account for the wall effect.

The damping function in the present model is taken to be a function of R_y , which is defined by

$$R_y = \frac{k^{1/2} y}{\nu}, \quad (12)$$

and takes the following form

$$f_\mu = [1 - \exp(-a_1 R_y - a_3 R_y^3 - a_5 R_y^5)]^{1/2} \quad (13)$$

where $a_1 = 1.5 \times 10^{-4}$, $a_3 = 5.0 \times 10^{-7}$, $a_5 = 1.0 \times 10^{-10}$. These constants are devised by comparing the performance of the model prediction and the DNS data for turbulent channel flow at $Re_\tau = 180$.

Near the wall, the shear stress $-\langle uv \rangle$ should behave as $O(y^3)$, as derived from equation (8). Since k is $O(y^2)$, we would require the damping function to have a near wall behavior of $O(y)$. From equation (12) and equation (13), it is seen that as $y \rightarrow 0$, $R_y \rightarrow 0$ as $O(y^2)$, which gives $f_\mu \rightarrow 0$ as $O(y)$. Thus, the near wall asymptotic behavior for the shear stress is satisfied. Far from the wall, R_y is large and $f_\mu \rightarrow 1$. The near wall eddy viscosity given by equation (11) then reduces to its counterpart for high Reynolds number flows given by equation (5).

Since R_y instead of y^+ is used as the independent variable in the damping function, the model could be expected to be applicable in more general flow situations including flows with separation and reattachment. It should be pointed out that the use of y in

the damping function makes the model non-Galelian invariant. In addition, in complicated geometry situations such as corner flows, the meaning of y is ambiguous. However, in the authors' view, these comments are more academic. In practical applications, the non-Galelian invariant will not be a problem through the use of a body fitted coordinate system with y denoting the direction normal to the wall. As for the corner flows, the ambiguity in y shows up only when it is very close to the corner, where k is very small, and the exact definition of y is not material.

The other effect in near wall turbulence is the effect of the inhomogeneity of the mean field which introduces a secondary source term in the dissipation equation. Combining all the above, the dissipation equation is finally written as

$$\dot{\epsilon} + U_j \epsilon_{,j} = [(\nu + \frac{\nu_T}{\sigma_\epsilon}) \epsilon_{,j}]_{,j} + (-C_{1\epsilon} \langle u_i u_j \rangle U_{i,j} - C_{2\epsilon} \epsilon) / T_t + E \quad (14)$$

where the time scale T_t is given by equation (9) and the secondary source term, E , is given by

$$E = \nu \nu_T U_{i,jk} U_{i,jk}. \quad (15)$$

This form was suggested by Jones and Launder³, and Shih⁵. The effect of E is confined to the buffer layer since away from the wall E becomes much smaller than the other terms in the dissipation equation.

Equations (6), (11) (14) are the $k - \epsilon$ equations proposed in this paper. The model constants, c_μ , $C_{1\epsilon}$, $C_{2\epsilon}$, σ_k , σ_ϵ , are the same as those in the Stanford $k - \epsilon$ Model. Away from the wall, the present model reduces to the Standard $k - \epsilon$ Model. Thus, it is only necessary to assess the performance of the model for near wall turbulence.

The boundary condition for ϵ on the wall is determined by applying equation (6) (the k equation) at the wall, which gives

$$\epsilon_w = \nu k_{,yy}.$$

In this study, the following boundary condition for ϵ , which is mathematically equivalent to the above but computationally much more robust, is used.

$$\epsilon_w = 2\nu \left(\frac{dk^{1/2}}{dy} \right)^2 \quad (16)$$

III. Numerical Aspects

Boundary layer approximation is used in the calculations shown below. An semi-implicit finite difference scheme is used to solve the momentum equation and the transport equations for k and ϵ . The coefficients for the convective terms are lagged one step in the marching direction and the source terms in the k and ϵ equations are linearized in such a way that numerical stability is ensured.

A variable grid spacing is used to resolve the sharp gradient near the wall. The grid distribution is controlled by $\delta y_i / \delta y_{i-1} = \alpha$. Both α and the total number of the grid, N , are varied to ensure the grid independence of the numerical results. The marching step size, δx , is also varied to ensure accuracy. In the test cases that follow, those parameters are changed such that the solution has a less than 1.0% error. Typically, the grids used are specified by $N = 150$ and $\alpha = 1.05$. However, it is found that the solution is not very sensitive to the number of the grid points as long as there are two points in $y^+ < 1$. Fig. 1 shows a calculation for the turbulent channel flow at $Re_\tau = 395$ with N varying from 30 to 150. It is seen that the results for different N are almost identical.

IV. RESULTS AND DISCUSSIONS

Turbulent channel flows at different Reynolds numbers and turbulent boundary layers with zero pressure gradient, favorable pressure gradient, adverse pressure gradient, and increasingly adverse pressure are calculated using the present model. The following shows the computational results compared with the available experimental data and data from direct numerical simulation. For some cases, the predictions of the Jones-Launder model and Chien's model⁹ are also shown. These two models are chosen because the Jones-Launder model is the first $k - \epsilon$ model for near wall turbulence while Chien's model is known to perform quite well for turbulent boundary layer flows.

Two dimensional fully developed channel flows were first chosen to validate the proposed model. These flows are attractive for model testing because they have self-similar solutions so that the initial conditions do not have to be accurately specified. These flows are very

simple and solutions can be found very efficiently; yet, the effects of the wall on turbulent shear flow are still present. In addition, DNS data providing detailed flow information is available for comparison. Computations are carried out for 2D fully developed turbulent channel flows at $Re_\tau = 180$ and $Re_\tau = 395$. Only the results for $Re_\tau = 395$ are shown. Fig. 2 shows the profiles of the mean velocity, shear stress, turbulent kinetic energy and the dissipation. Both the dependent variable and the independent variables are represented in wall units by normalization through u_τ and ν . The predictions of the Jones-Launder model and Chien's model are also shown. These predictions are compared with the DNS data. It is found that the present model predicts accurately the peak value of turbulent energy and the location of maximum value of the dissipation rate. (It should be at the wall.) Overall, the present model gives a better prediction.

Like the 2D fully developed channel flows, turbulent boundary layer flows over a flat plate also give a self-similar solution. Thus, arbitrary profiles could be used as the initial conditions and the solution would develop into its similarity form. In our case, constant values are assigned to the velocity, turbulent energy and the dissipation rate. The exact values for the initial profiles are immaterial as long as the turbulent boundary gets generated. The boundary conditions used are that, at the free stream, the velocity reaches that of the freestream, while the turbulent energy and the dissipation rate are set to zero. Fig. 3 shows the predicted velocity profile, turbulent energy, shear stress, and dissipation rate at $Re_\theta = 1410$. The DNS data of Spalart¹⁰ is also shown. Again, the predictions from the Jones-Launder model and Chien's model are shown in the same figure for comparison. The results by the present model are found to be better.

The computations were also carried out for larger Reynolds number cases and the comparison is made between the model prediction and the experimental results of Wieghardt and Willmann¹¹. Fig. 4 shows the results of the skin friction coefficient as a function of Re_θ . The skin friction by DNS at $Re_\theta = 1410$ by Spalart¹⁰ is also shown in this figure. Overall, the present model gives prediction of about 8% more than the experiment. It should be pointed out that for low Reynolds numbers situations, the skin friction from the experiment is lower than that from the DNS. For example, at $Re_\theta = 1410$, $C_f(\text{DNS}) = 4.13 \cdot 10^{-3}$, while

the experiment gives $C_f(\text{EXP}) = 3.97 \cdot 10^{-3}$, which is 4% lower than DNS. The present model predicts $C_f(\text{Present}) = 4.08 \cdot 10^{-3}$. In Fig. 5, the velocity profile at $Re_\theta = 8900$ is presented. It is seen that the present model prediction and the experiment agrees quite well.

When the turbulent boundary layer is subject to a pressure gradient, the similarity solution ceases to exist. In this case, accurate description of the initial conditions for the velocity profile and the profiles of turbulence quantities (turbulent energy and dissipation rate) are very important. While experiment could provide the velocity profile at the upstream location, information on the turbulence quantities is hardly available. In this study, the issue of the initial condition is dealt with in the following manner. We assume that the turbulent boundary layer develops under zero pressure gradient until it passes into the working section of the wind tunnel, where the experimental measurements are made. The connecting point between this virtual flat plate boundary layer and the real boundary layer with the pressure gradient is determined by the value of Re_θ which is found by the experiment.

The boundary conditions are specified in the same way as in the case of a flat plate boundary layer. At the wall, both the velocity and the turbulent energy are equal to zero while the dissipation rate is given by equation (16). At the free stream, zero values are assigned to the turbulent energy and its dissipation rate. The mean velocity approaches that of the free stream, which is determined by the experiment and is related to the pressure gradient of the flow.

In the present study, the turbulent boundary layer with favorable pressure gradient studied by Herring and Norbury¹¹, the turbulent boundary layer under adverse pressure gradient studied by Bradshaw¹¹, and the turbulent boundary layer under increasingly adverse pressure gradient studied by Samuel and Joubert¹² are calculated, respectively. The first two are the test cases for the 1968 Stanford Conference on Turbulent Boundary Layers¹¹ and the last one is a test case in the 1981-82 Stanford Conference on Complex Turbulent Flows¹³. The results of the calculation are shown below and the comparison is made with the experimental data in each of the cases.

Herring and Norbury¹¹ studied the development of a turbulent boundary layer under a favorable pressure gradient. At the first point of the working section of the experiment, $Re_\theta = 3400$. Thus, a flat plate boundary at $Re_\theta = 3400$ is used to provide the initial conditions. With the initial conditions given, the calculation of the boundary layer is then carried out downstream. The result for the skin friction coefficient is shown in Fig. 6, and the result for the mean velocity at $x = 4\text{ft}$ is shown in Fig. 7. The distances, x and y , are in physical units while the skin friction and the velocity are normalized by the freestream velocity at the streamwise location under consideration. It is seen that both the velocity and the skin friction are well predicted.

The Bradshaw¹¹ experiment simulated in this paper is a flow where the turbulent boundary layer develops under an adverse pressure gradient. The first point where the velocity profile (and hence Re_θ) is known is at $x = 2\text{ft}$, where $Re_\theta = 7810$. The experiment clearly indicates that the pressure gradient is quite strong at $x = 2\text{ft}$. (The strongest over all the working section for this experiment.) Thus, the specification of the initial conditions based on a flat plate boundary layer may not be very accurate. This is evidenced by Fig. 8a which shows the velocity profile from the experiment and the velocity profile from the flat plate boundary calculation. The difference between the two is quite substantial. Our prediction then carries some error with it due to the specification of the initial conditions; however, we hoped that this error would decrease as the calculation marches downstream. This is indeed found to be true. Fig. 8b shows the velocity profiles at $x = 4\text{ft}$. It is clear that the model gives quite good results even though the initial conditions are not accurately prescribed. The distribution of the skin friction coefficient is shown in Fig. 9. As in the case of the favorable pressure gradient, both x and y are shown in physical units, while the skin friction and the velocity are normalized by the freestream velocity at the streamwise location under consideration.

In the Samuel and Joubert flow, the turbulent boundary layer develops under increasingly adverse pressure gradient. During the 1981-82 Stanford Conference on Complex Turbulent Flows¹³, it was found that this flow is very difficult to predict. Since then, it has become a strong test case for turbulence models.

The initial conditions are specified at $x = 0.855\text{m}$, where $Re_\theta = 5470$. First, the predicted skin friction is shown in Fig. 10 with the experimental values. The variation of the skin friction coefficient with x is well-captured. However, the predicted value is higher than the experiment result by a constant amount of 3.0×10^{-4} , which amounts to about 11% at $x = 0.855$. It should be mentioned that at $x = 0.855$ where the pressure gradient is very small, one would expect that the experimental result for the skin friction coefficient would be the same as that for the flat plate boundary layer at the same value of Re_θ , found by the experiment of Wiegardt and Willmann, for example. However, it is seen that the result for this case is smaller than that of Wiegardt and Willmann by 1.4×10^{-4} , which amounts to 5%. The velocity profile at $x = 1.76\text{m}$ is shown in Fig. 11. The turbulence quantities (shear stress and the turbulent energy) at $x = 1.79\text{m}$ are shown in Fig. 12 and Fig. 13, respectively.

V. CONCLUSION

We have presented a $k - \epsilon$ model for wall bounded flows which is free from the three deficiencies we pointed out in the introduction. First, the proposed model uses the same set of model constants as that used in the Standard $k - \epsilon$ Model and away from the wall the proposed model will reduce to the Standard $k - \epsilon$ Model. Thus, the proposed model would be applicable in both near wall turbulence and high Reynolds number turbulence. Second, the proposed model uses a time scale which has the Kolmogorov time scale as its lower bound. By using this time scale to reformulate the dissipation equation, the singularity in the standard dissipation equation is removed as the wall is approached and the equation can be integrated to the wall. This renders the introduction of pseudo-dissipation unnecessary. Third, the proposed model uses R_ν instead of y^+ as its independent variable in the damping function. This allows the model to be used in more complicated flow situations, flows with separation, for example.

Turbulent channel flows at different Reynolds numbers and turbulent boundary layers with/without pressure gradient are calculated using the present model. At low Reynolds number, the comparison between the DNS data and the present model is found to be excel-

lent. At higher Reynolds numbers, the velocity profiles are well-predicted. The predicted skin friction coefficient is within 8% of that of the experiment for a flat plate boundary layer, and is in an excellent agreement with the boundary layer under favorable pressure gradient (Herring and Norbury flow). For adverse pressure gradient cases, the predicted skin friction coefficient is less than 18% higher for the Bradshaw flow and for the Samuel and Joubert flow.

It should be mentioned that the model is computationally robust. Arbitrary initial profiles can be used for turbulent channel flows and flat plate boundary layers when similarity solutions exist. The predicted solution is also found to be quite insensitive to the number of grid points.

ACKNOWLEDGEMENT

Dr. Charles Feiler of ICOMP, NASA Lewis Research Center read an earlier draft. The DNS data used was kindly made available to us by Dr. N. Mansour of NASA Ames Research Center. Help from Dr. A.T. Hsu of Center for Modeling of Turbulence and Transition, NASA Lewis Research Center on numerical computation is also acknowledged.

REFERENCES

¹Launder, B.E., and Spalding, D.B., "The Numerical Computation of Turbulent Flow," *Computer Methods in Applied Mechanics and Engineering* Vol. 3, 1974, pp 269-289.

²Rodi, W., *Turbulence Models and Their Application in Hydraulics*, Book Pub. of International Association for Hydraulic Research, Delft, the Netherlands, 1980.

³Jones, W.P., and Launder, B.E., "The Calculation of Low-Reynolds Number Phenomena with a Two-Equation Model of Turbulence," *International Journal of Heat and Mass Transfer*, Vol.16, 1973, pp 1119-1130.

⁴Patel, V.C., Rodi, W., and Scheuerer, G., "Turbulence Models for Near-Wall and Low-Reynolds Number Flows: a Review," *AIAA Journal*, Vol. 23, 1985, pp 1308-1319.

⁵Shih, T.H., "An Improved $k - \epsilon$ Model for Near-Wall Turbulence and Comparison with Direct Numerical Simulation," *NASA TM*, 103211, 1990.

⁶Lang, N.J., and Shih, T.H., "A Critical Comparison of Two Equation Turbulence Models," *NASA TM*, 105237, 1991.

⁷Hanjalic, K., and Launder, B.E., "Contribution towards a Reynolds-stress Closure for Low-Reynolds-number turbulence," *Journal of Fluid Mechanics*, Vol. 74, 1976, pp 593-610.

⁸Durbin, P., "Near-Wall Turbulence Closure Modeling with 'Damping Function'," *Theoretical and Computational Fluid Dynamics*, Vol. 3, 1991, pp 1-13.

⁹Chien, K.Y., "Predictions of Channel and Boundary Layer Flow with a Low-Reynolds-Number Turbulence Model," *AIAA Journal*, Vol. 20, 1982, pp 33-38.

¹⁰Spalart, P.R., "Direct Simulation of a Turbulent Boundary Layer up to $Re_\theta = 1410$," *Journal of Fluid Mechanics*, Vol. 187, 1988, pp 61-98.

¹¹Coles, D.E., and Hirst, E.A., "Computation of Turbulent Boundary Layers-1968 AFOSR-IFP-Stanford Conference," Vol. 2, Stanford University, 1969.

¹²Samuel, A.E., and Joubert, P.N., "A boundary Layer Developing in an Increasingly Adverse Pressure Gradient," *Journal of Fluid Mechanics*, Vol. 66, 1974, pp 481-505.

¹³Kline, S.J., Cantwell, B.J., and Lilley, G.M., "1980-81 AFOSR-HTTM-Stanford Conference on Complex Turbulent Flows," Stanford University, 1981.

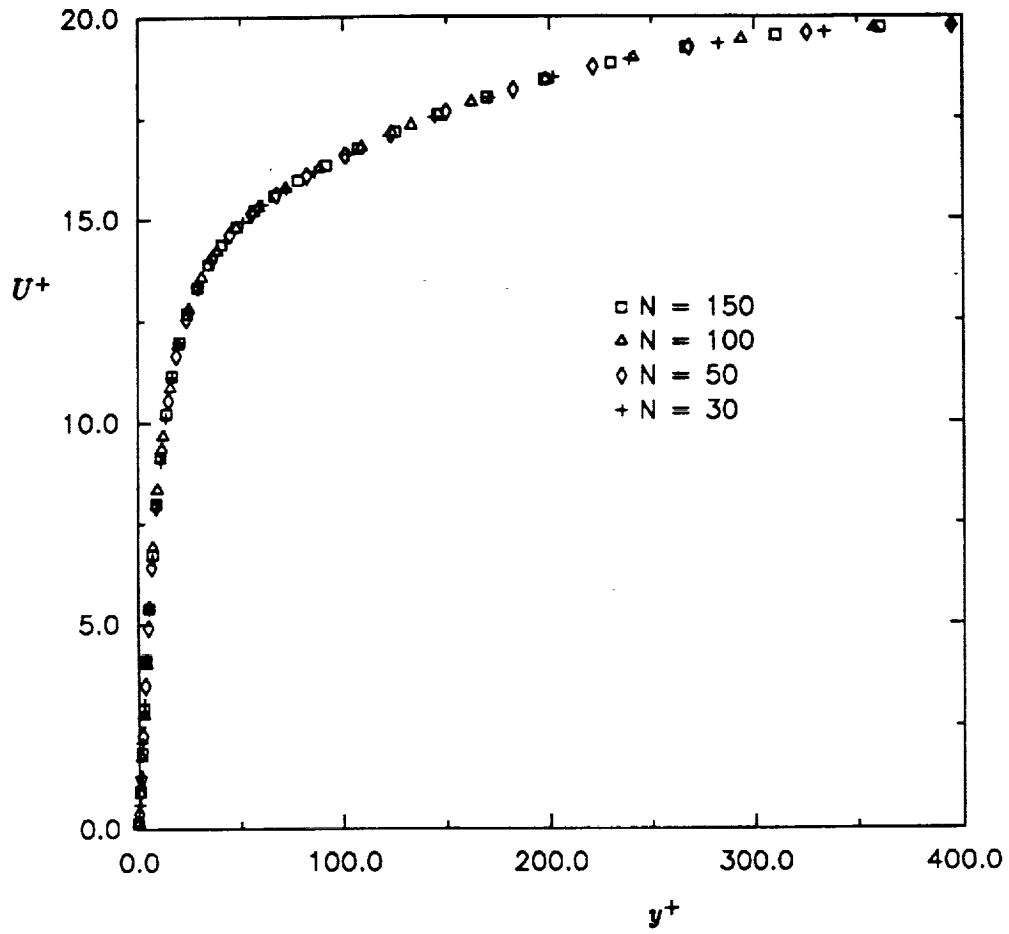


Fig. 1: Mean velocity profile found by different number of grid points.

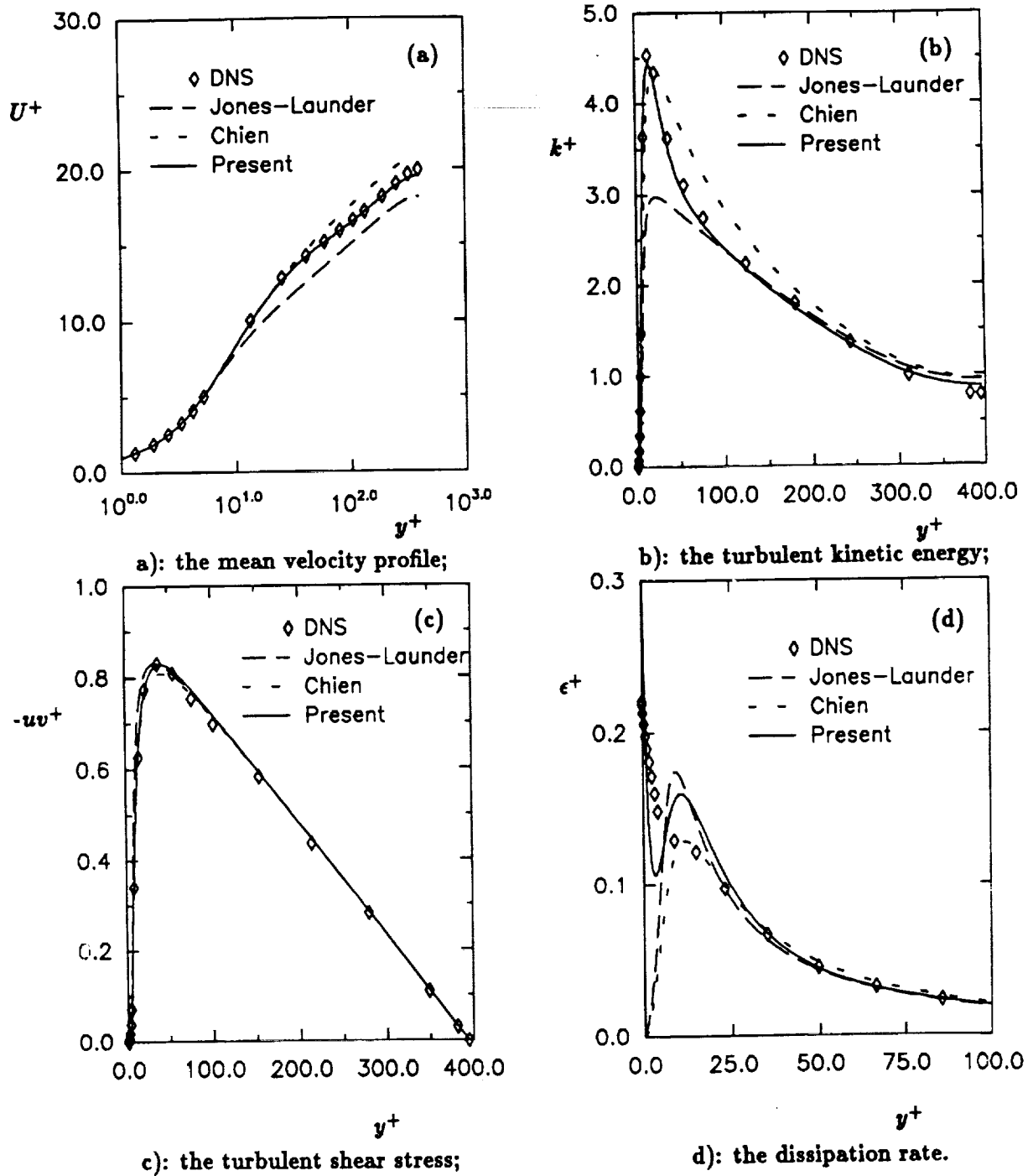


Fig. 2: Turbulent channel flow at $Re_\tau = 395$

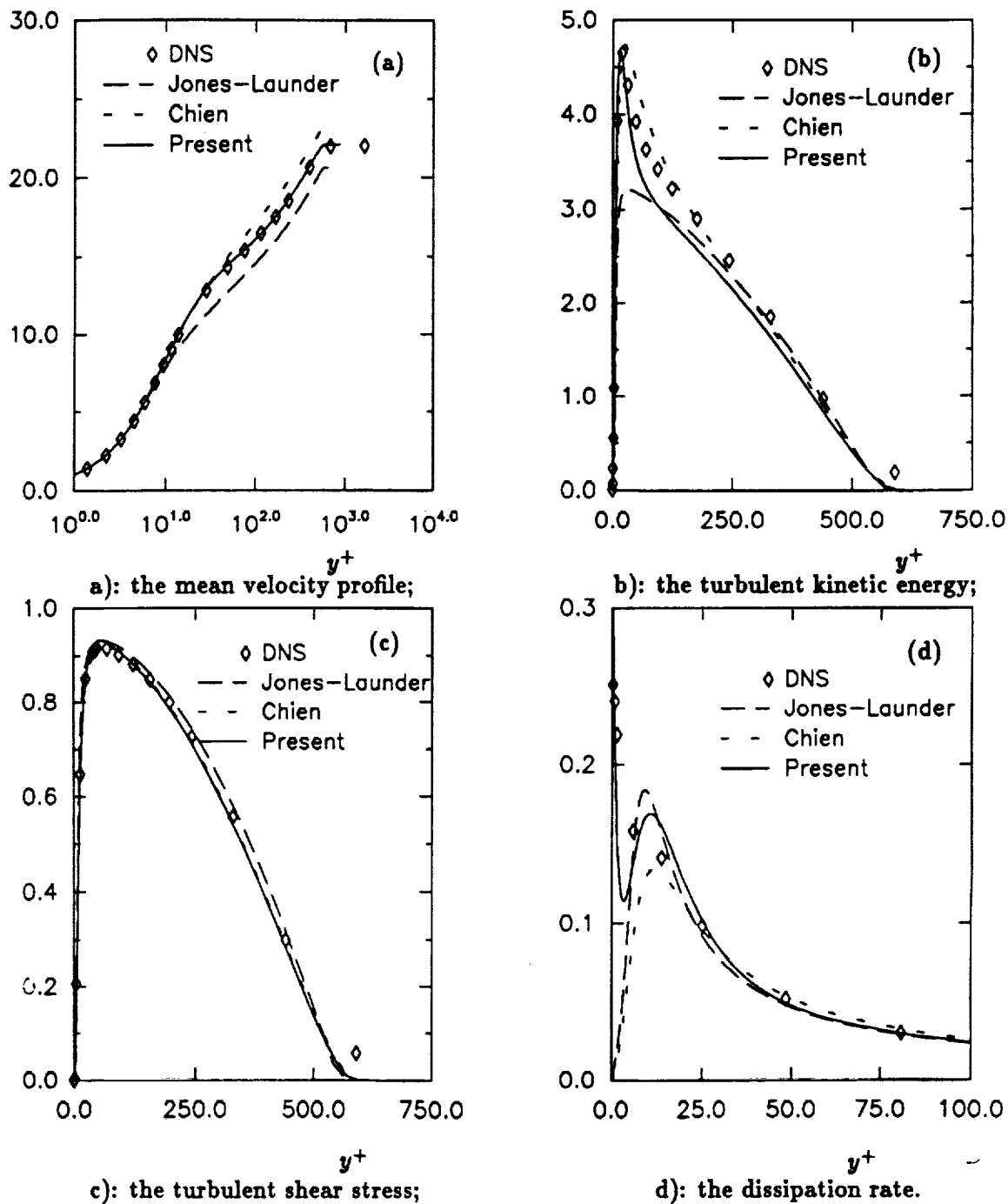


Fig. 3: Turbulent flat plate boundary layer at $Re_\theta = 1410$

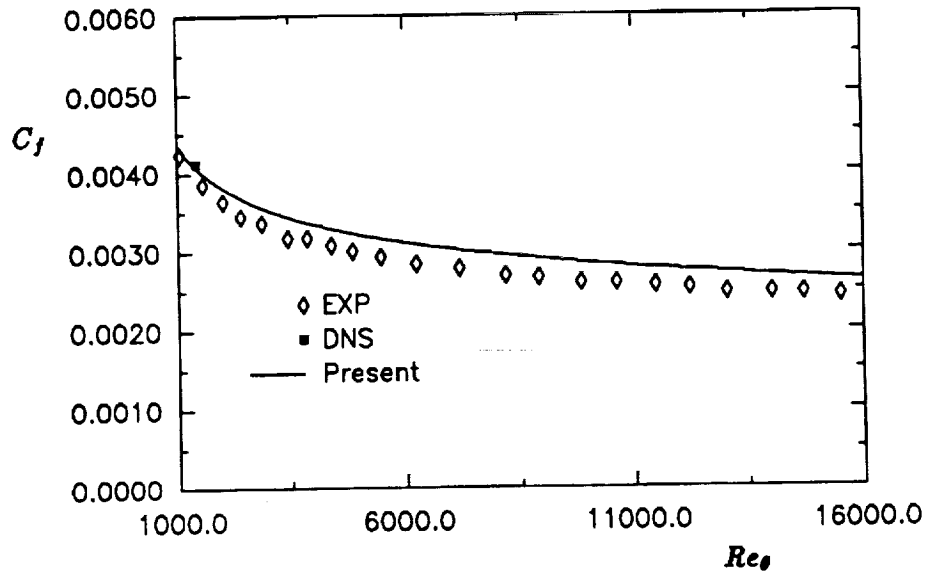


Fig. 4: Skin friction distribution for turbulent flat plate boundary layer.

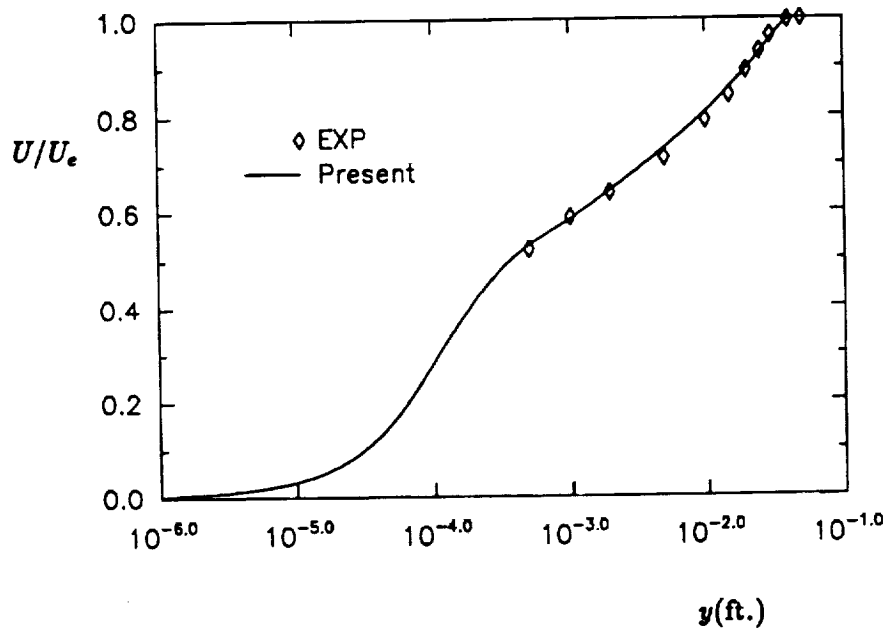


Fig. 5: Velocity profile for turbulent flat plate boundary layer at $Re_\theta = 8900$.

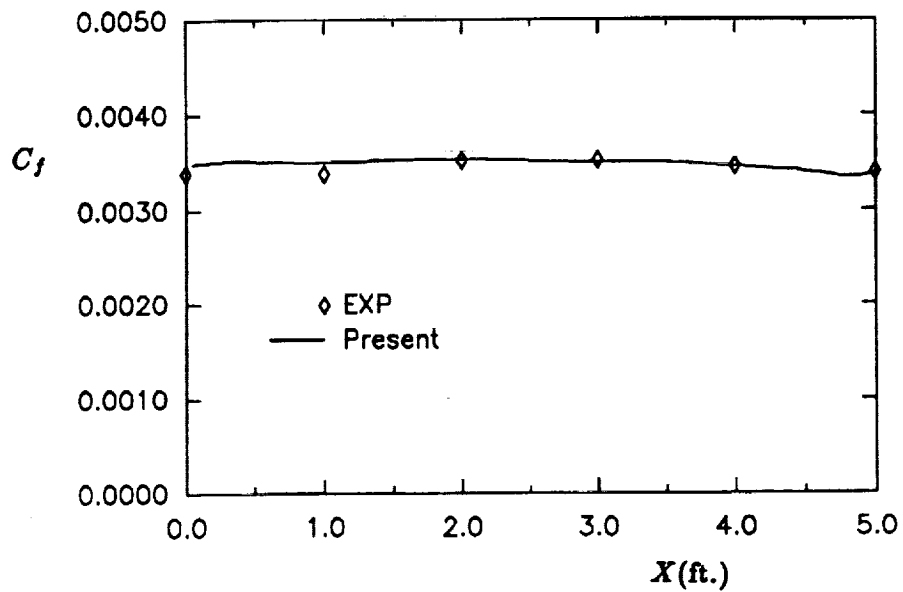


Fig. 6: Skin friction distribution for Herring and Norbury flow.

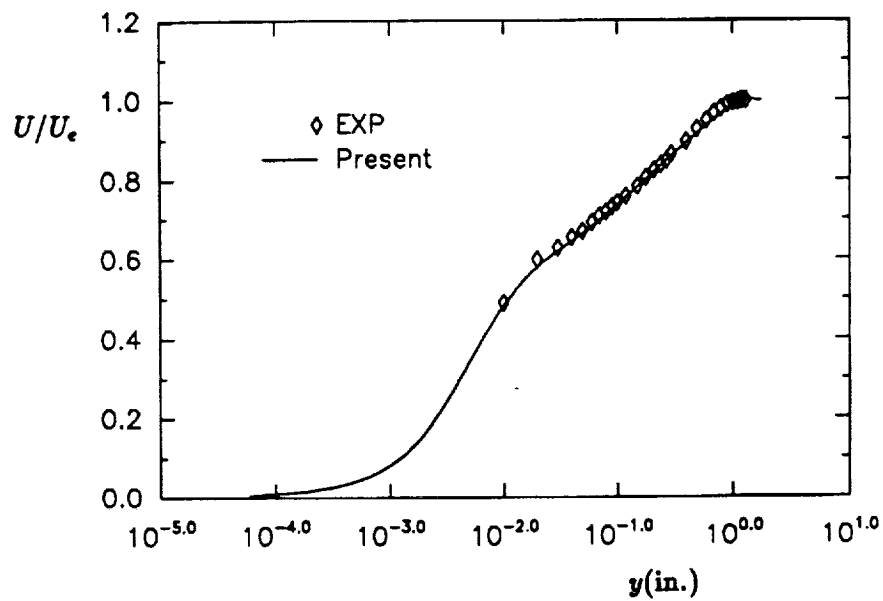


Fig. 7: Velocity profile for Herring and Norbury flow at $x = 4\text{ft.}$

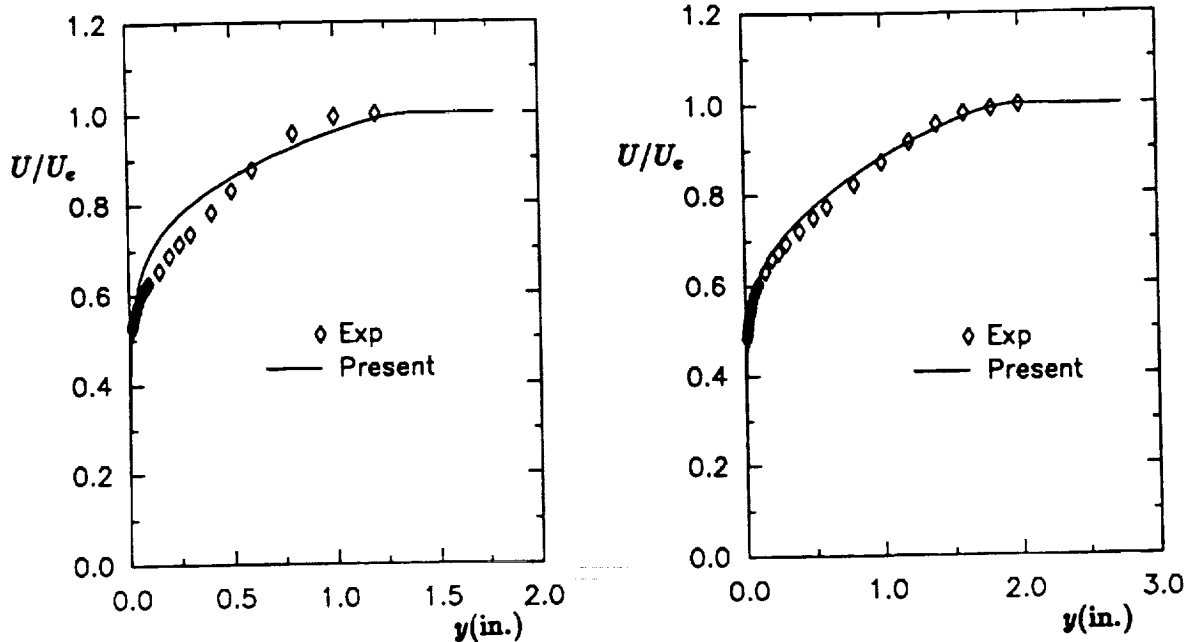


Fig. 8: Velocity profile for Bradshaw flow. a): $x = 2\text{ft}$; b): $x = 4\text{ft}$.

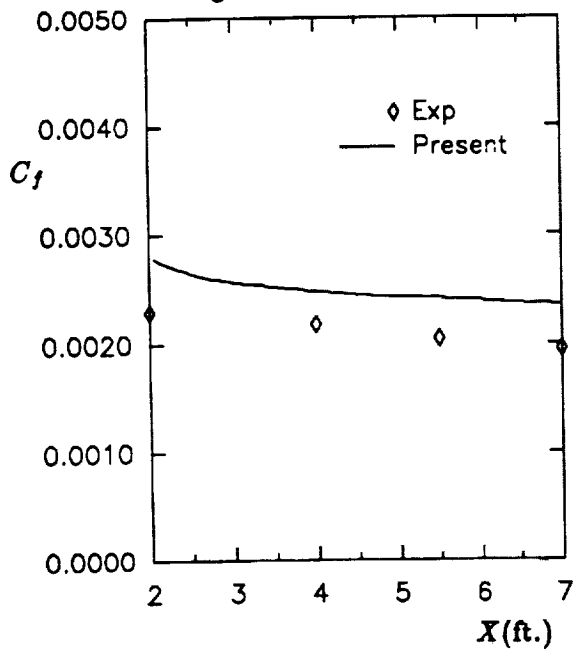


Fig. 9: Skin friction distribution for Bradshaw flow.

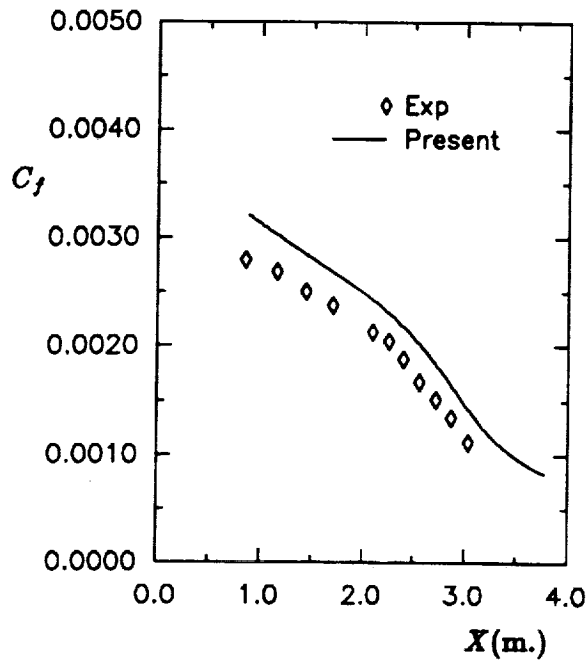


Fig. 10: Skin friction distribution for Samuel and Joubert flow.

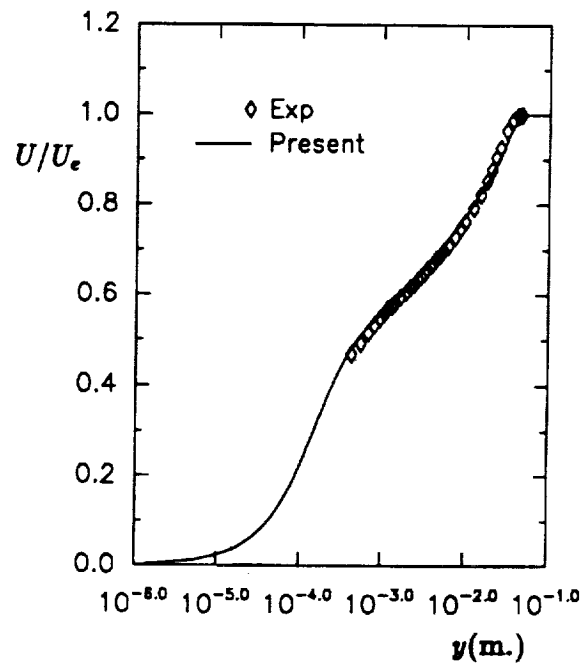


Fig. 11: Velocity profile for Samuel and Joubert flow at $x = 1.76m$.

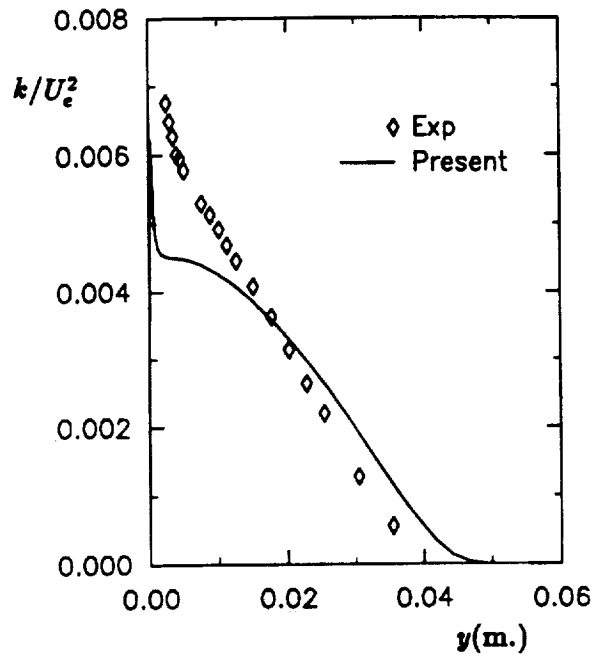


Fig. 12: Turbulent energy for Samuel and Joubert flow at $x = 1.79\text{m}$.

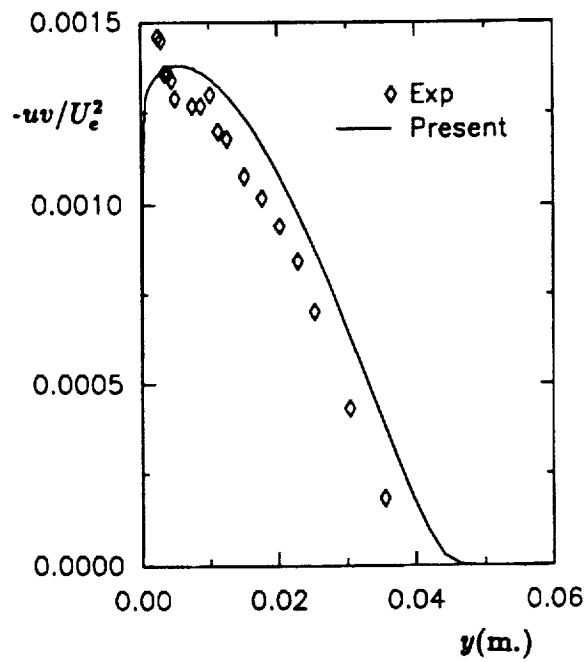


Fig. 13: Turbulent shear stress for Samuel and Joubert flow at $x = 1.79\text{m}$.

REPORT DOCUMENTATION PAGE

Form Approved
OMB No. 0704-0188

Public reporting burden for this collection of information is estimated to average 1 hour per response, including the time for reviewing instructions, searching existing data sources, gathering and maintaining the data needed, and completing and reviewing the collection of information. Send comments regarding this burden estimate or any other aspect of this collection of information, including suggestions for reducing this burden, to Washington Headquarters Services, Directorate for Information Operations and Reports, 1215 Jefferson Davis Highway, Suite 1204, Arlington, VA 22202-4302, and to the Office of Management and Budget, Paperwork Reduction Project (0704-0188), Washington, DC 20503.

1. AGENCY USE ONLY (Leave blank)	2. REPORT DATE January 1992	3. REPORT TYPE AND DATES COVERED Technical Memorandum	
4. TITLE AND SUBTITLE A New Time Scale Based <i>k-ε</i> Model for Near Wall Turbulence		5. FUNDING NUMBERS WU-505-62-21	
6. AUTHOR(S) Z. Yang and T.H. Shih		8. PERFORMING ORGANIZATION REPORT NUMBER E-7194	
7. PERFORMING ORGANIZATION NAME(S) AND ADDRESS(ES) National Aeronautics and Space Administration Lewis Research Center Cleveland, Ohio 44135-3191		10. SPONSORING/MONITORING AGENCY REPORT NUMBER NASA TM-105768 ICOMP-92- 11; CMOTT-92-07	
9. SPONSORING/MONITORING AGENCY NAMES(S) AND ADDRESS(ES) National Aeronautics and Space Administration Washington, D.C. 20546-0001		11. SUPPLEMENTARY NOTES Z. Yang and T.H. Shih, Institute for Computational Mechanics in Propulsion and Center for Modeling of Turbulence and Transition, NASA Lewis Research Center, Cleveland, Ohio; (work funded by Space Act Agreement C-99066-6). ICOMP Program Director, Louis A. Povinelli, (216) 433-5818.	
12a. DISTRIBUTION/AVAILABILITY STATEMENT Unclassified - Unlimited Subject Category 34		12b. DISTRIBUTION CODE	
13. ABSTRACT (Maximum 200 words) A <i>k-ε</i> model is proposed for wall bounded turbulent flows. In this model, the eddy viscosity is characterized by a turbulent velocity scale and a turbulent time scale. The time scale is bounded from below by the Kolmogorov time scale. The dissipation equation is reformulated using this time scale and no singularity exists at the wall. The damping function used in the eddy viscosity is chosen to be a function of $R_y = \frac{k^{1/2}y}{\nu}$ instead of y^+ . Hence, the model could be used for flows with separation. The model constants used are the same as in the high Reynolds number standard <i>k-ε</i> model. Thus, the proposed model will be also suitable for flows far from the wall. Turbulent channel flows at different Reynolds numbers and turbulent boundary layer flows with and without pressure gradient are calculated. Results show that the model predictions are in good agreement with direct numerical simulation and experimental data.			
14. SUBJECT TERMS <i>k-ε</i> model; Near wall turbulence; Turbulent boundary layers; Turbulent time scale			15. NUMBER OF PAGES 22
17. SECURITY CLASSIFICATION OF REPORT Unclassified			16. PRICE CODE A03
18. SECURITY CLASSIFICATION OF THIS PAGE Unclassified	19. SECURITY CLASSIFICATION OF ABSTRACT Unclassified	20. LIMITATION OF ABSTRACT	